

# Order–Disorder Phase Transitions in Tetrathioorthoesters of Group IV Elements $X(\text{SCH}_3)_4$ , $X = \text{C}, \text{Si}, \text{Ge}, \text{Sn}$

Hartmut Fuess\* and Roman Strauss

Fachgebiet Strukturforschung, Fachbereich Materialwissenschaft, Technical University Darmstadt, Petersenstr. 23, 64287 Darmstadt, Germany

Keisuke Kimura and Michio Sorai

Faculty of Science, Osaka University, Toyonaka 560, Japan

Received: October 13, 1997; In Final Form: February 4, 1998

The order–disorder phase transition of tetrathioorthoesters of the elements of group IV with the general formula  $X(\text{SCH}_3)_4$  and  $X = \text{C}, \text{Si}, \text{Ge}, \text{Sn}$  was studied by differential thermal analysis, X-ray diffraction, and  $^1\text{H}$  NMR measurements. Whereas a disordered phase was observed in a broad temperature range for  $\text{C}(\text{SCH}_3)_4$ , this phase gradually decreases with increasing radius of the central atom. No disordered phase was observed for  $\text{Sn}(\text{SCH}_3)_4$ . A model for the completely ordered and partially disordered phases of  $\text{C}(\text{SCH}_3)_4$  is proposed.

## 1. Introduction

Order–disorder phase transitions in the solid state are often closely connected with a rather compact form of the constituent molecules. Therefore, spherical or elliptical molecules with mainly hydrogen atoms on the surface are potential candidates for order–disorder phase transitions and the formation of so-called plastic phases was already stated about 60 years ago.<sup>1</sup> Many globular, spherical molecules are known to form plastic phases, like  $\text{CH}_4$ ,  $\text{SiH}_4$ ,  $\text{GeH}_4$ , or  $\text{CCl}_4$ , whereas no such phase was observed for  $\text{SiF}_4$  and  $\text{SiCl}_4$ . A classical case for the formation of a plastic phase is adamantane  $\text{C}_4(\text{CH}_2)_6$ , but the urotropin molecule  $\text{N}_4(\text{CH}_2)_6$  with a similar molecular structure does not form a plastic phase. It seems, therefore, that a globular spherical form of a molecule is not sufficient for the formation of the plastic phase.

According to Timmermans (1938),<sup>1</sup> a plastic phase is characterized by two transitions, one at  $T_m$  the melting point, the other  $T_{\text{I–II}}$  for the order–disorder transition. Phase I is the disordered phase and phase II the ordered one. In some cases further transitions are observed. The thermodynamic criterion for the existence of a plastic phase is a low entropy of melting  $\Delta S_{\text{I–m}}$ . An empirical value for a dimensionless quantity  $\Delta S_{\text{I–m}}/R = 2.5$  may be given as a rule of thumb. The entropy at the order–disorder transition is, however, fairly high. From thermodynamics the entropy is therefore the most important quantity for the formation of the plastic solid state.

Owing to the long-range order of the centers of the molecules and the absence of order in the orientation of the molecule, a high symmetry (cubic or hexagonal) is found in phase I. The modifications observed at lower temperature have a considerably lower symmetry and the phase transition  $\text{I} \rightarrow \text{II}$  is accompanied by a considerable hysteresis. The more or less free rotation of molecules in a solid is the result of the possibility of forming an almost spherical shape when rotating about an axis. Empirical rules for the prediction of plastic phases were given by Nitta.<sup>2</sup>

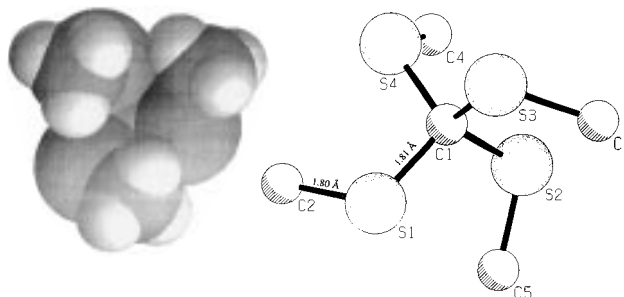


**Figure 1.** Molecular dimensions of  $\text{C}(\text{SCH}_3)_4$ : (left) model showing the spherical molecule; (right) atomic arrangement and mean distances.

(i) For crystals built of tetrahedral molecules, the simplest case is methane and its derivatives. The thioesters treated here may be considered as derivatives of methane. (ii) For crystals consisting of quasi- or pseudooctahedral molecules, these molecules essentially form a rotational ellipsoid. Examples are hexasubstituted ethane, like hexachlorethane  $\text{Cl}_3\text{C–CCl}_3$  or tetramethylbutane  $(\text{CH}_3)_3\text{C–C}(\text{CH}_3)_3$ . (iii) Examples of molecular crystals with spherical units are cyclobutane, cyclopropane, hexane, and adamantane.

The title compounds may be derived from neopentane  $\text{C}(\text{CH}_3)_4$  or the homologous  $\text{X}(\text{CH}_3)_4$ , with  $X = \text{Si}, \text{Ge}, \text{Sn}$ , by the substitution of the methyl groups by thiomethyl groups  $\text{SCH}_3$ . The questions to be asked concern the influence of the central atom and the changes between the methyl and the  $\text{S}(\text{CH}_3)_4$  derivatives. Whereas neopentane  $\text{C}(\text{CH}_3)_4$  is a classical plastic crystal, the homologous  $\text{Si}(\text{CH}_3)_4$  only forms a metastable plastic phase<sup>3</sup> and no plastic phase was observed for  $\text{Ge}(\text{CH}_3)_4$ ,  $\text{Sn}(\text{CH}_3)_4$ , and  $\text{Pb}(\text{CH}_3)_4$ .<sup>4–6</sup>

Oriental disorder for  $\text{C}(\text{SCH}_3)_4$  has already been reported by Backer and Perdok.<sup>7</sup> They determined the phase diagram and transition enthalpies. Furthermore, crystal structures of the different modifications were proposed.<sup>7–9</sup> The dimensions of the molecule are given in a schematic way in Figure 1.

Nothing is known in the literature of the thermodynamics and crystal structure of  $\text{X}(\text{SCH}_3)_4$ ;  $X = \text{Si}, \text{Ge}, \text{Sn}$ . Vibrational spectra of the four orthothioesters were given by Ypenburg and

\* To whom correspondence should be addressed. Telephone: 06151/162298. Fax: 06151/166023. E-mail: dd9n@hrzpub.tu-darmstadt.de.

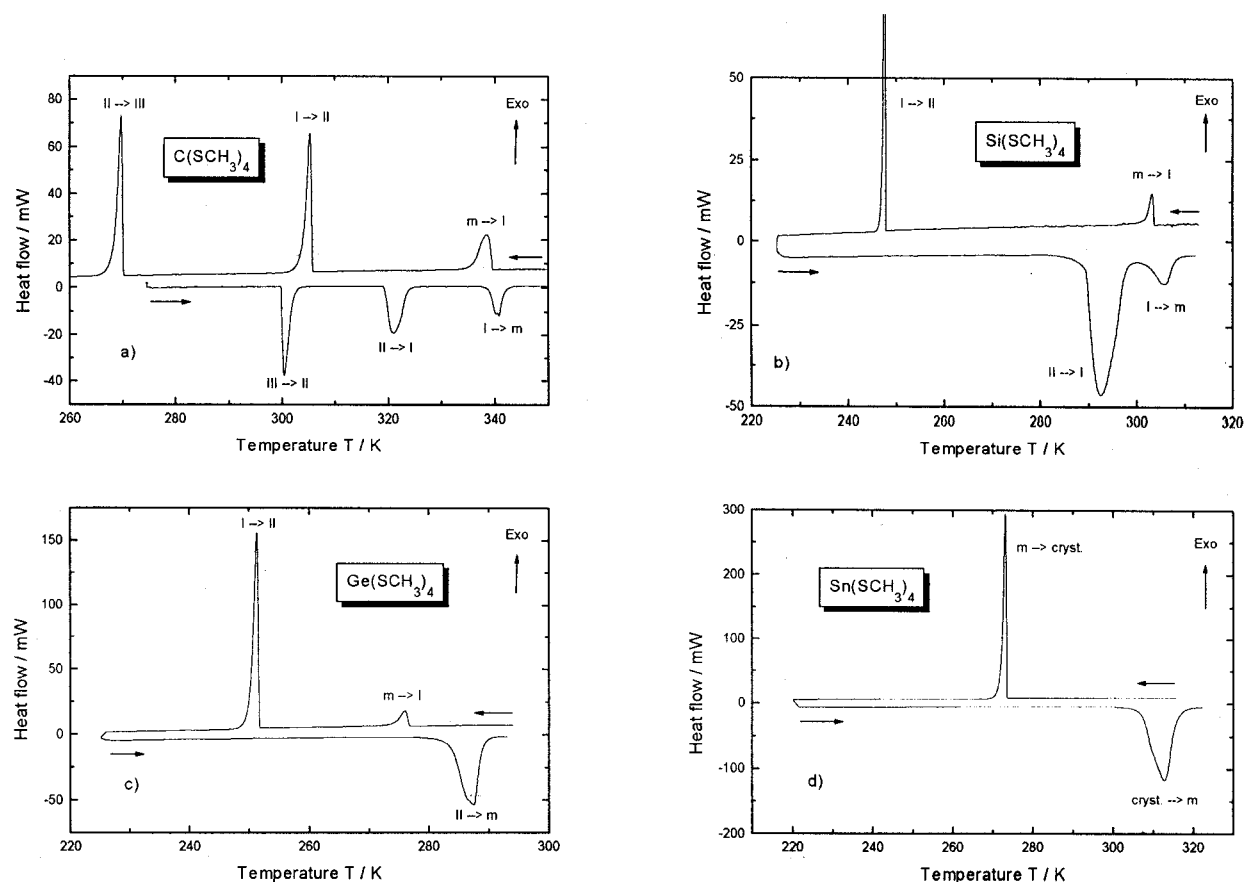


Figure 2. Differential scanning calorimetry measurements. Heating and cooling curves are presented for four compounds.

Gerding<sup>10</sup> and <sup>1</sup>H NMR data by Cumper et al.<sup>11</sup> and van dem Berghé.<sup>12</sup> In addition, photoelectron emission spectra were reported for C(Si(CH<sub>3</sub>)<sub>3</sub>)<sub>4</sub>.<sup>13</sup>

## 2. Experimental Section

The four compounds were prepared according to techniques reported in the literature.<sup>7,14</sup>

The thermodynamic measurements were performed with an instrument constructed and described by Strauss (1996)<sup>14</sup> and a SETARAM DSC121. The former was essentially used for temperatures below room temperature, the second for those above. The DSC instruments were carefully calibrated by a mixture of ice and water and the known melting points of several organic compounds. Complete calibration data were registered for terephthalic acid and hexamethylbenzene. The reproducibility of the temperatures was  $\pm 0.3$  K. The error derived from the calibration was 0.6 K for the range  $234 < T < 395$  K, but it is higher for lower temperatures. The maximum error in the enthalpy measurements is 5%. The temperatures derived from  $c_p$  experiments have an error of 0.1 K due to calibration. X-ray powder diffraction was carried out with a STOE-STADIP diffractometer and Cu K $\alpha$  radiation. The pattern were registered by position-sensitive detectors (6° and 40° aperture, respectively). A furnace ( $300 \text{ K} < T < 1300 \text{ K}$ ) and a cryostream ( $100 \text{ K} < T < 300 \text{ K}$ ) system were available.

The nuclear resonance measurements (NMR) were performed on a spectrometer with a regenerative oscillator (Robinson type). A constant frequency (8.1 MHz) and a variable field from  $20 \times 10^4$  to  $100 \times 10^4$  T were applied. The samples were encapsulated in glass capillaries and were mounted in a Dewar, which was continuously floated by a gas. The temperature was

registered by a copper–constantan thermocouple, and the temperature was constant within 1 K.

## 3. Results

**3.1. Differential Scanning Calorimetry.** Three phase transitions were observed for C(Si(CH<sub>3</sub>)<sub>3</sub>)<sub>4</sub> in the temperature range  $260 \text{ K} < T < 350 \text{ K}$ . Below the melting point  $T_{I \rightarrow m} = 339.4 \text{ K}$ , an optical isotropic phase I is stable. The low value of the reduced melting entropy  $\Delta S_{I \rightarrow m}/R = 1.2$  is representative of a plastic phase. Between 298.3 and 319.6 K a crystalline phase with birefringence is observed that transforms below  $T_{II \rightarrow III}$  into an ordered low-temperature phase. The values of the transition enthalpies  $\Delta H_{III \rightarrow II} = 7.4 \text{ kJ/mol}$  and  $\Delta H_{II \rightarrow I} = 7.5 \text{ kJ/mol}$  (Table 1) indicate a two-stage process from the disordered high-temperature phase to the ordered low-temperature one.

For the tetramethylester of tetraorthosilicon Si(Si(CH<sub>3</sub>)<sub>3</sub>)<sub>4</sub>, only one solid–solid transition at  $T_{II \rightarrow I}$  was observed and the solid phase below the melt is a uniaxial anisotropic system. All thermodynamic data (Table 1) indicate a plastic phase for the temperature range  $289.9 \text{ K} < T < 301.9 \text{ K}$ .

The thermal analysis of the germanium compound does not show a solid–solid transition on heating but only a melting point. On cooling ( $1 \text{ K min}^{-1}$ ) a plastic phase is observed between 276.8 and 251.8 K. Temperature-dependent measurements were carried out in order to discuss the stability of the plastic phase. These results will be described below.

No indication of a plastic phase has been observed for the tetramethylester of the tetraorthotinacid Sn(Si(CH<sub>3</sub>)<sub>3</sub>)<sub>4</sub>. The rather broad peak observed on heating may indicate two events that are only separated by a small temperature interval. The high values of melting enthalpy and entropy do not, however, favor

TABLE 1: Thermodynamic Data from DSC Measurements for  $X(\text{SCH}_3)_4$ ,  $X = \text{C, Si, Ge, Sn}^a$ 

	III $\rightarrow$ II			II $\rightarrow$ I			I $\rightarrow$ m			rate
	$T_i$	$\Delta H$	$\Delta S/R$	$T_i$	$\Delta H$	$\Delta S/R$	$T_i$	$\Delta H$	$\Delta S/R$	
C	2908.3	7.4	3.0	319.6	7.5	2.8	339.4	3.5	1.2	1.0 H
	269.4	-7.3	-3.3	306.0	-6.8	-2.7	339.8	-3.4	-1.2	0.75 C
	296.23	7.0	2.87	318.76	7.29	2.75	339.89	3.3	1.17	CAL
Si				289.8	11.6	4.8	301.9	1.8	0.7	0.5 H
				248.0	-10.2	-5.0	303.7	-1.8	-0.7	0.5 C
				288.6	11.63	4.79	304.5	2.19	0.81	CAL
Ge							284.1	14.2	6.0	1.0
				251.8	-11.7	-5.6	276.8	-1.6	-0.7	1.0 C
Sn							307.5	24.1	9.4	1.0 H
							273.7	-23.2	-10.2	1.0 C

<sup>a</sup> Given are the transition temperatures  $T_i$  [K], the enthalpy  $\Delta H$  [kJ/mol<sup>-1</sup>], and the reduced entropy  $\Delta S/R$  for the phase transitions. DSC values for heating (H) and cooling (C) are given. Additional values are added from  $c_p$  measurements (CAL). A negative sign stands for an exothermic process. For the temperatures of the DSC experiments a maximum error of 0.6 K for  $234 \text{ K} < T < 395 \text{ K}$  is experimentally obtained from calibration. The enthalpy values have an error of 5%. The error of the calorimetric measurements is  $\pm 0.1 \text{ K}$  for  $T_i$  and 1% for  $\Delta H$ .

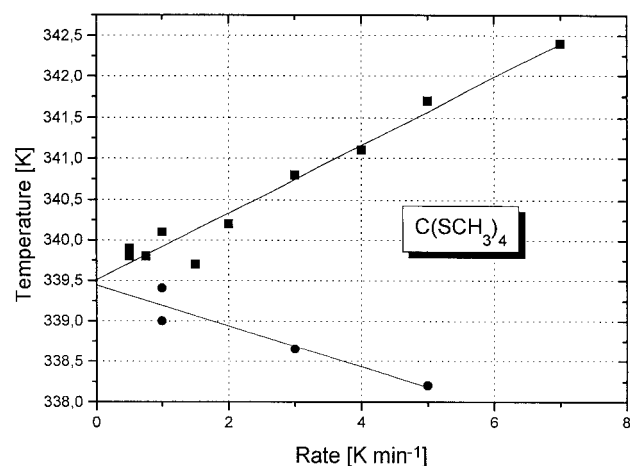


Figure 3. Melting (●) and freezing (◆) temperature as a function of heating and cooling rate for  $\text{C}(\text{SCH}_3)_4$ .

the existence of a plastic phase. The DSC curves for the four compounds are shown in Figure 2.

**3.2. Rate-Dependent Thermal Analysis.** Phase transitions in the solid phase of plastic crystals often show a temperature hysteresis. The solidification temperatures are, on the other hand, hardly influenced by the cooling or heating rate. Therefore, studies with different rates were performed. The melting and solidification temperatures for  $\text{C}(\text{SCH}_3)_4$  are presented in Figure 3. All crystallization temperatures are above the melting temperatures, and the difference increases with increasing rate. This difference is attributed to a temperature gradient in the sample. The melting temperature is thus obtained by extrapolating to a rate of  $0 \text{ K min}^{-1}$ . Similar observations were made for the two solid–solid transitions, and the values of transition temperatures in Table 1 were obtained by extrapolation.

**3.3 Specific Heat.** The specific heat has been measured in the temperature range from 15 to 360 K in an adiabatic calorimeter. No corrections for vapor pressure were applied, since the vapor pressure is very small and therefore does not influence the enthalpy of evaporation. This is justified, since the pressure is 0.5 mbar below the melting point and no difference was found between phases II and I.

Figure 4 shows the temperature dependence of  $c_p$ . The curve displays a sharp increase between 15 and 100 K, which is due to a thermal excitation of  $\text{CH}_3$  groups around the S–C bond.

Values of the specific heat were derived and compared with earlier results.<sup>7</sup> The considerable differences are explained by the method, depression of melting point, used by Backer et al.<sup>7</sup>

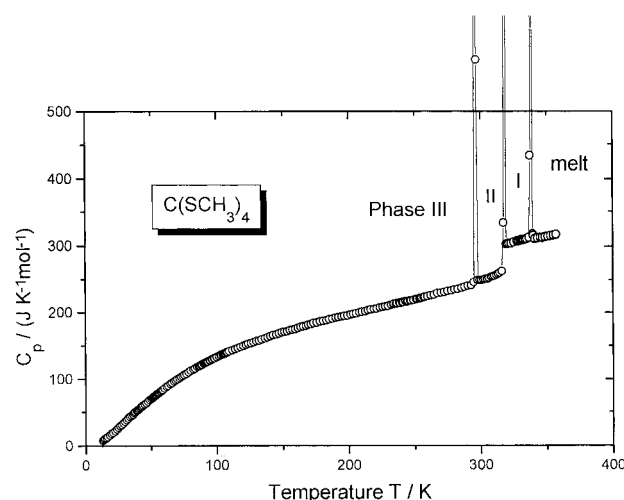


Figure 4. Molar specific heat for  $\text{C}(\text{SCH}_3)_4$  in the temperature range  $15 \text{ K} < T < 360 \text{ K}$ .

The temperature dependence of the excess enthalpy and excess entropy is given in Figure 5. The almost equal values for the transitions III  $\rightarrow$  II and II  $\rightarrow$  I are remarkable. They are related to a two-step process of the transition from an ordered to a completely disordered crystal.

Figure 6 presents the molar specific heat  $c_p$  for  $\text{Si}(\text{SCH}_3)_4$  as a function of temperature for 15–320 K. Compared with the DSC measurements, two additional small peaks at  $T = 115.2$  and  $274.6 \text{ K}$  were detected. It is not clear whether those are additional peaks or whether they are due to impurities. Compared with the carbon compound, the melting peak is broader and the maximum considerably smaller. This broad peak is considered as a premelting phenomenon. Since this may be due to impurities, the substance was examined by fractional melting and a purity of 99.23 mol % was obtained. Table 1 gives the thermodynamic data from the DSC and from the specific heat measurements.

**3.4. X-ray Diffraction.** The plastic phases of  $\text{C}(\text{SCH}_3)_4$ ,  $\text{Si}(\text{SCH}_3)_4$  and  $\text{Ge}(\text{SCH}_3)_4$  were studied by powder X-ray diffraction. The pattern for  $\text{C}(\text{SCH}_3)_4$  is presented in Figure 7 which only shows three reflections. Similar patterns were obtained for the homologous compounds of Si and Ge. The reflections were indexed in the cubic crystal system with a body-centered cell in  $Im\bar{3}m$ . The lattice constants derived are displayed in Table 2. It should be stated that  $Im\bar{3}m$  is the highest possible symmetry, but space groups with lower symmetry cannot be excluded. Temperature-dependent measurements

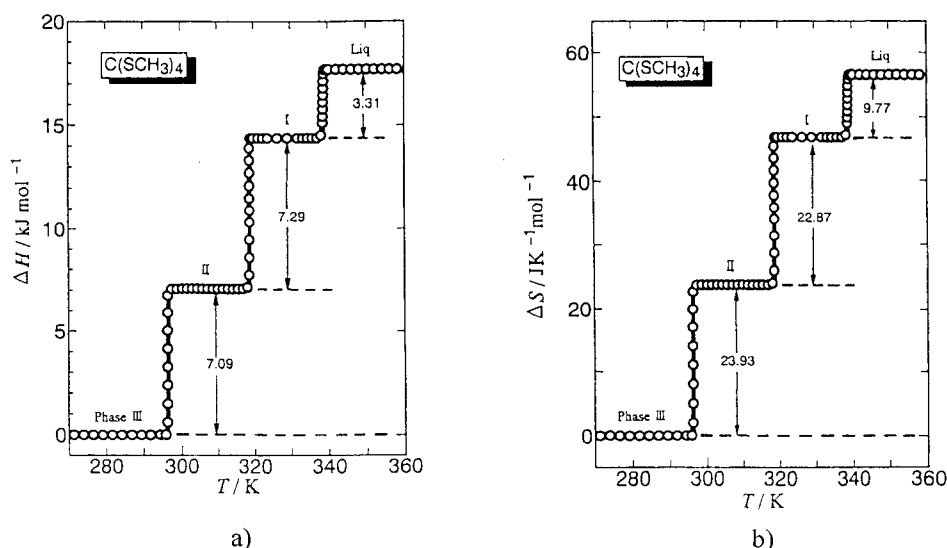


Figure 5. (a) Excess enthalpy and (b) Excess entropy for  $C(SCH_3)_4$ .

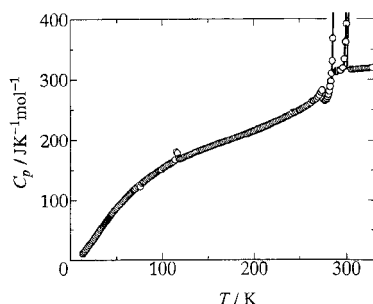


Figure 6. Molar specific heat for  $Si(SCH_3)_4$  for the temperature range 15 K <  $T$  < 330 K.

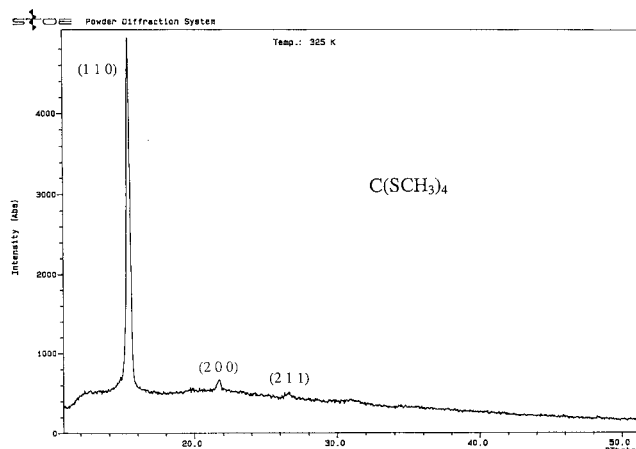


Figure 7. X-ray pattern for the plastic phase of  $C(SCH_3)_4$  at 325 K.

TABLE 2: Lattice Constants  $a_0$  in pm and Thermal Expansion Coefficients for the Plastic Phases

	space group	$T / K$	$a_0 / \text{pm}$	$\alpha \times 10^4 [K^{-1}]$
$C(SCH_3)_4$	$Im\bar{3}m$	325	816.7	3.41
$Si(SCH_3)_4$	$Im\bar{3}m$	270	842.0	2.09
$Ge(SCH_3)_4$	$Im\bar{3}m$	273	846.4	2.81

have been carried out, and the linear expansion coefficient  $\alpha_T$  was derived (Figure 8). The considerable increase in the lattice constants between  $C(SCH_3)_4$  and the homologous compounds is remarkable. X-ray studies of the low-temperature phases are in progress.

**$^3H$  NMR Spectroscopy.** The  $^1H$  NMR signals were converted to the second moment, which is given as

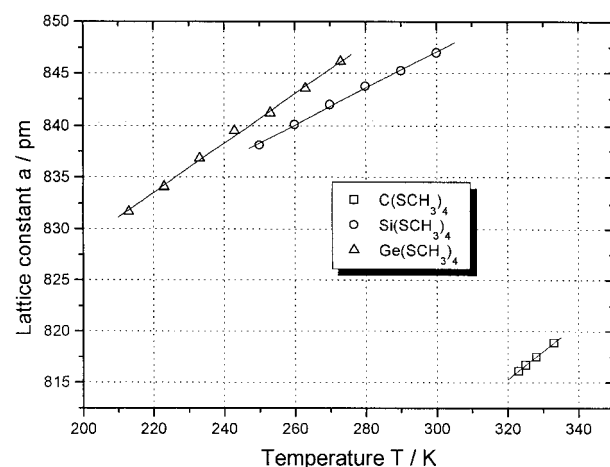


Figure 8. Temperature dependence of lattice constants for  $X(SCH_3)_4$ ,  $X = C, Si, Ge$ , in the plastic state.

$$M_2 = \int (\omega - \omega_0)^2 F(\omega) d\omega / \int F(\omega) d\omega$$

$F(\omega)$  is the intensity function, and  $\omega_0$  is the frequency at the line maximum or the zero position of the derivative of the intensity.

The line width  $\Delta B$  is defined as the distance between the extrema of the derived signal. The temperature dependence of  $\Delta B$  and  $M_2$  for  $C(SCH_3)_4$  is shown in the range 150 K <  $T$  < 340 K. An additional point (not shown in Figure 9) has been measured at 77 K. Both values remain almost constant between 77 K and the transition temperature III  $\rightarrow$  II and a value of  $7.5 \times 10^{-8} T^2$  for  $M_2$  is observed. The transition temperature is marked by a considerable decrease to a value of  $0.65 \times 10^{-8} T^2$  in phase II.

The second moment contains some information on the geometrical arrangement of the spins in the crystal. According to van Vleck,<sup>15</sup> the second moment may be calculated in the case where only one kind of nuclei is present. Since contributions of  $^{13}C$ ,  $^{33}S$ ,  $^{29}Si$ , and  $^{13}Ge$  were neglected, this assumption is valid in our case.

Typical values in plastic crystals are on the order of  $1 \times 10^{-8} T^2$ , and they are basically due to intermolecular interactions. This corresponds to the assumption that all spins of a molecule are located in its center. The resulting expression is then obtained according to Boden.<sup>16</sup>

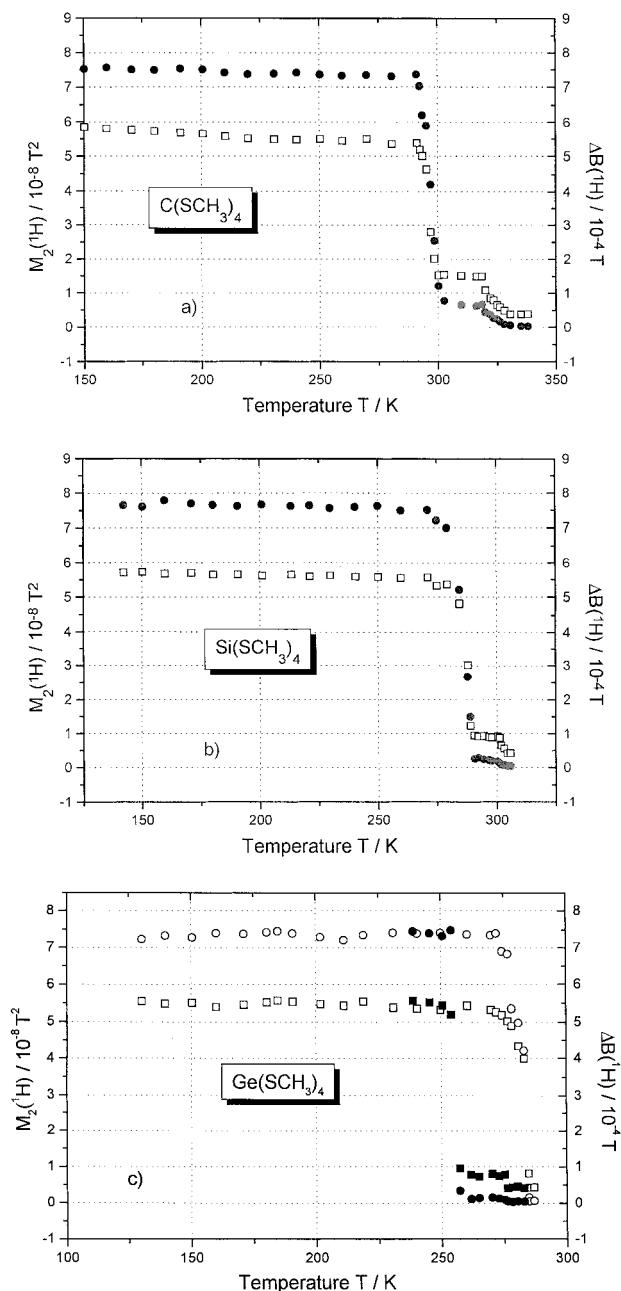


**Figure 9.** Line width  $\Delta B$  ( $\square$ ) and second moment  $M_2$  ( $\bullet$ ) as derived from  $^1\text{H}$  NMR spectroscopy: (a) for  $\text{C}(\text{SCH}_3)_4$ ; (b) for  $\text{Si}(\text{SCH}_3)_4$ ; (c) for  $\text{Ge}(\text{SCH}_3)_4$ , line width  $\Delta B$  ( $\square$  heating,  $\blacksquare$  cooling) and  $M_2$  ( $\circ$  heating,  $\bullet$  cooling).

$$M_2 = \frac{6}{5} g^2 \beta^2 I(I+1) n^{-1} \sum_{i < j} r_{ij}^{-6}$$

$n$  is number of resonating spins,  $g$  the nuclear  $g$  factor,  $\beta$  the nuclear magneton,  $I$  the nuclear quantum number, and  $r_{ij}$  the distance between nuclei.

The lattice sums are easily derived for the lattice types that are observed in plastic phases. For a body-centered cubic ( $Im\bar{3}m$ ) lattice the value for the lattice sum is  $r = 29.05a_0$  with  $a_0$  the lattice constant. At the melting point  $M_2 \rightarrow 0$  the intermolecular dipolar interactions are averaged owing to translational diffusion.

The intramolecular distances were calculated on the basis of van der Waals values of 100 pm for H and 200 pm for  $\text{CH}_3$  and tetrahedral angles  $\angle\text{SCS} = \angle\text{HCS} = 109^\circ 28'$  and  $\angle\text{CSC}$

**TABLE 3: Calculated and Observed Values of the Second Moment<sup>a</sup>**

	$M_2$ (rigid)	$M_2$ (methyl rotation)	$M_2$ (molecular rotation)
intrameth	22.4	5.6	0
intramol	0.3	0.3	0
intermol	1.9	1.0	0.42
total	24.6	6.9	0.42
expt	7.5	0.45	

<sup>a</sup> The Values for  $M_2$  (methyl rotation) correspond to phase II, the values for molecular rotation to phase I.

$\approx \text{HSC} = 98^\circ 52'$ . This leads to a mean distance between the methyl groups of 448 pm.

For a comparison with experimental values the second moment was calculated for a general molecular orientation in the plastic phase and for a rigid molecule in a rigid lattice. The calculated values are given in Table 3.

The predicted one even at 77 K is far from the predicted value for a rigid molecule; that means the rotation of  $\text{CH}_3$  about  $\text{S}-\text{CH}_3$  is not yet frozen in and the experimental value of  $7.5 \times 10^{-8} \text{ T}^2$  corresponds to free rotation of methyl groups in phase III. The value of  $0.65 \times 10^{-8} \text{ T}^2$  in phase II has to be explained by an additional dynamical process. Perdok et al.<sup>8,9</sup> proposed a rotation of the  $\text{CS}_4$  tetrahedra that is, however, in contradiction to our caloric data (see Discussion section). A possible explanation is a hindered rotation of the thiomethyl group about the  $\text{C}-\text{SCH}_3$  bond. The value for the plastic phase agrees well with a model of free rotation. Further studies for the temperature range below 150 K should give additional information on the temperature dependence.

The experimental results for  $\text{Si}(\text{SCH}_3)_4$  may be explained in a similar way. The values at 77 K correspond to an ordered low-temperature phase with rotating methyl groups. The second moment remains constant up to the phase transition and drops sharply, corresponding to an isotropic reorientation of the molecules, which results in a value of  $0.34 \times 10^{-8} \text{ T}^2$  without diffusion. It drops further near the melting point owing to additional diffusion (Figure 9b).

Since the transition in  $\text{Ge}(\text{SCH}_3)_4$  is monotropic, the values of  $\Delta B$  and  $M_2$  were measured on cooling and heating. The value at  $T = 77 \text{ K}$  corresponds to the other two compounds. It remains constant up to the melting point. On cooling, however, a small moment of  $M_2 = 0.34 \times 10^{-8} \text{ T}^2$  is observed for the plastic phase, which indicates additional diffusion in the rotator phase. A sharp increase is observed at the transition (Figure 9c).

#### 4. Discussion

The single-crystal structure determination of Perdok and Terpstra<sup>8</sup> for  $\text{C}(\text{SCH}_3)_4$  indicated tetragonal symmetry for the two low-temperature phases. Space group  $I4/mmm$  was attributed to phase II and space group  $P4_21c$  for phase III. The space group of the plastic phase was given as  $Im\bar{3}m$ , in agreement with our results. Ypenburg et al.<sup>10</sup> measured IR and RAMAN spectra and derived molecular configurations for the three phases. They determined the molecular symmetry as  $D_{2d}$  and  $S_4$  in phase I and in the melt. On the basis of these results and the previously described structure determination of Perdok et al.,<sup>7,8</sup> they derived a possible model for the motion in the three phases. According to them in phase III (below 296.3 K), only the  $\text{CH}_3$  group rotates about the  $\text{S}-\text{C}$  axes. In phase II two orientations are possible for each methyl group with respect to the central  $\text{CS}_4$  tetrahedron. Furthermore each  $\text{CS}_4$  tetrahe-



**TABLE 4: Entropy at Phase Transition [ $\text{J K}^{-1} \text{mol}^{-1}$ ] for  $\text{C}(\text{SCH}_3)_4$ <sup>a</sup>**

	calorimetric data		
	expt	literature <sup>8,10</sup>	model, this work
III $\rightarrow$ II	23.93	28.82	23.05
II $\rightarrow$ I	22.87	13.48	19.25
I $\rightarrow$ m	9.77	9.13	9.13

<sup>a</sup> Expt: calorimetric data. Literature values calculated according to a model proposed by Ypenburg et al.<sup>10</sup> based on structural data from Perdok et al.<sup>8</sup>

dron may perform 90° jumps about the  $\text{C}_3$  axis of the  $\text{CS}_4$  tetrahedron. The calculated entropy for the transition III  $\rightarrow$  II is therefore  $\Delta S_{\text{III} \rightarrow \text{II}} = R \ln(2 \times 2^4) = 28.82 \text{ J mol}^{-1} \text{ K}^{-1}$ , whereas our measurements (Table 1) give a value of  $23.93 \text{ J mol}^{-1} \text{ K}^{-1}$ . The model for phase I is described by three equivalent positions of each methyl group with respect to the  $\text{CS}_4$  tetrahedron. The entropy for the transition II  $\rightarrow$  I is then calculated as  $\Delta S_{\text{II} \rightarrow \text{I}} = R \ln(3^4/2^4) = 13.48 \text{ J mol}^{-1}$ . Our measurements indicate  $\Delta S_{\text{II} \rightarrow \text{I}} = 22.87 \text{ J mol}^{-1} \text{ K}^{-1}$ . The calculated values based on the model given by Ypenburg et al.<sup>10</sup> disagree with our precise calorimetric data. We therefore propose a new, modified model for the structures of phases III and II and the resulting transitions.

In phase III the central  $\text{CS}_4$  tetrahedron is fixed and the  $\text{CH}_3$  groups have only one position with respect to this tetrahedron. A rotation of the  $\text{CH}_3$  groups seems likely, since the value of the second moment for the rigid molecule ( $M_2 = 22.4 \times 10^{-8} \text{ T}^2$ ) is not observed. The solid–solid transition III  $\rightarrow$  II is characterized by the freedom of each methyl group to occupy two positions partially whereas the  $\text{CS}_4$  tetrahedron remains stable. The entropy calculated for that situation for  $\Delta S_{\text{III} \rightarrow \text{II}} = R \ln(2^4) = 23.05 \text{ J mol}^{-1} \text{ K}^{-1}$  is in good agreement with the experimental value. The transition II  $\rightarrow$  I presents the 90° jump–rotation of the  $\text{CS}_4$  tetrahedron and three possible orientations of each  $\text{CH}_3$  group, thus resulting in  $\Delta S_{\text{II} \rightarrow \text{I}} = R \ln(2 \times 3^4/2^4) = 19.25 \text{ J mol}^{-1} \text{ K}^{-1}$ , in agreement with the measurements. Table 4 summarizes the experimental and calculated  $\Delta S$  values.

The basic difference between the two models consists of the onset of the jump rotation of the  $\text{CS}_4$  tetrahedron. According to the literature model,<sup>10</sup> this reorientation does already exist in phase II, whereas we propose it only for phase I. For the space group proposed for phase II ( $I4/mmm$ ), a rotation of the  $\text{CS}_4$  tetrahedron is required but the measured entropy  $\Delta S_{\text{III} \rightarrow \text{II}}$  is too small to explain such a motion. The symmetry of phase II should therefore be lower, and we propose space group  $P4$  or  $I4$  for phase II. Additional X-ray work is therefore mandatory. The low entropy of melting  $\Delta S_{\text{I} \rightarrow \text{m}} = 9.77 \text{ J mol}^{-1}$

$\text{K}^{-1}$  is in agreement with general observations for plastic crystals and is near  $R \ln 3 = 9.13 \text{ J mol}^{-1} \text{ K}^{-1}$ , the value from the general gas theory. Therefore,  $\Delta S_{\text{I} \rightarrow \text{m}}$  may be explained by the loss of long-range order alone. The entropies for the two transitions in the solid state  $\Delta S_{\text{III} \rightarrow \text{I}}$  and  $\Delta S_{\text{II} \rightarrow \text{I}}$  are similar. Both are characterized by undercooling phenomena, an indication of first-order transitions related to changes in the crystal structure.

## 5. Conclusion

On the basis of thermodynamic data, previous literature values of vibrational spectroscopy and X-ray structure results, a model for the reorientation of  $\text{C}(\text{SCH}_3)_4$  in the three solid phases is proposed. A redetermination of the crystal structures of the low-temperature phases III and II is required in order to fully support the model. A similar pattern is observed for  $\text{Si}(\text{SCH}_3)_4$ , but phase II is either very small or absent. Therefore, the model for phase I is supposed to be identical to  $\text{C}(\text{SCH}_3)_4$  and the low-temperature phase is supposed to have an order similar to that of phase III of the carbon compound. Further work on the solid solution  $\text{C}(\text{SCH}_3)_4$ – $\text{Si}(\text{SCH}_3)_4$  is in progress and may contribute to the explanation of the reorientation processes.

**Acknowledgment.** This work has been initiated by the late Professor Alarich Weiss. Financial support of the Deutsche Forschungsgemeinschaft and Fonds der Chemischen Industrie is gratefully acknowledged.

## References and Notes

- (1) Timmermans, J. *J. Chim. Phys.* **1938**, *35*, 331.
- (2) Nitta, I. *Z. Kristallogr.* **1959**, *112*, 234.
- (3) Atake, T.; Chihara, H. *Chem. Phys. Lett.* **1978**, *56*, 330.
- (4) Guthrie, G. B.; McCullough, J. P. *J. Phys. Chem. Solids* **1961**, *18*, 53.
- (5) Harada, M.; Atake, T.; Chihara, H. *J. Chem. Thermodyn.* **1977**, *9*, 523.
- (6) Smith, G. W. *J. Chem. Phys.* **1965**, *42*, 4229.
- (7) Backer, H. J.; Perdok, W. G. *Recl. Trav. Chim. Pays-Bas* **1943**, *62*, 533.
- (8) Perdok, W. G.; Terpstra, P. *Recl. Trav. Chim. Pays-Bas* **1946**, *65*, 493.
- (9) Perdok, W. G. *Helv. Chim. Acta* **1947**, *30*, 1782.
- (10) Ypenburg, J. W.; Gerding, H. *Recl. Trav. Chim. Pays-Bas* **1972**, *91*, 1117.
- (11) Cumper, C. W. N.; Melnikoff, A.; Vogel, A. I. *J. Chem. Soc. B* **1966**, 874.
- (12) van den Berghe, E. V.; van der Kelen, G. P. *J. Organomet. Chem.* **1976**, *122*, 329.
- (13) Kobayashi, M.; Gleiter, R.; Coffen, D. L.; Bock, H.; Schulz, D. L. W.; Stein, U. *Tetrahedron* **1977**, *33*, 433.
- (14) Strauss, R. Ph.D. Thesis, Technical University, Darmstadt, Germany, 1996.
- (15) van Vleck, J. H. *Phys. Rev.* **1948**, *74*, 1168.
- (16) Boden, N. In *The plastically crystalline state*; Sherwood, J. N., Ed.; John Wiley & Sons: Chichester, 1979; p 147.